Silicon Microfabricated Column with Microfabricated Differential Mobility Spectrometer for GC Analysis of Volatile Organic Compounds

ARTICLE *in* ANALYTICAL CHEMISTRY · JANUARY 2006

Impact Factor: 5.64 · DOI: 10.1021/ac051216s · Source: PubMed

7 AUTHORS, INCLUDING:

Erkinjon G. Nazarov
Draper Laboratory
93 PUBLICATIONS **2,255** CITATIONS

SEE PROFILE

Silicon Microfabricated Column with Microfabricated Differential Mobility Spectrometer for GC Analysis of Volatile Organic Compounds

Gordon R. Lambertus,† Cory S. Fix,† Shaelah M. Reidy,† Ranaan A. Miller,‡ David Wheeler,‡ Erkinjon Nazarov,‡ and Richard Sacks*,†

Department of Chemistry, University of Michigan, Ann Arbor, Michigan 48109, and Sionex Corporation, 8-A Preston Court, Bedford, Massachusetts 01730

A 3.0-m-long, 150-μm-wide, 240-μm-deep channel etched in a 3.2-cm-square silicon chip, covered with a Pyrex wafer, and coated with a dimethyl polysiloxane stationary phase is used for the GC separation of volatile organic compounds. The column, which generates ~5500 theoretical plates, is temperature-programmed in a conventional convection oven. The column is connected through a heated transfer line to a microfabricated differential mobility spectrometer. The spectrometer incorporates a ^{63}Ni source for atmospheric-pressure chemical ionization of the analytes. Nitrogen or air transport gas (flow 300 cm^3/min) drives the analyte ions through the cell. The spectrometer operates with an asymmetric radio frequency (RF) electric field between a pair of electrodes in the detector cell. During each radio frequency cycle, the ion mobility alternates between a high-field and a low-field value (differential mobility). Ions oscillate between the electrodes, and only ions with an appropriate differential mobility reach a pair of biased collectors at the downstream end of the cell. A compensation voltage applied to one of the RF electrodes is scanned to allow ions with different differential mobilities to pass through the cell without being annihilated at the RF electrodes. A unique feature of the device is that both positive and negative ions are detected from a single experiment. The combined microfabricated column and detector is evaluated for the analysis of volatile organic compounds with a variety of functionalities.

Miniaturized and microfabricated instruments for gas chromatography (GC) are under development in several laboratories.[1−6] These instruments are of interest because of their very small size, weight, and resource requirements and are intended for on-site analysis. Completely autonomous instruments for remote sensing will use atmospheric-pressure air as carrier gas,[7−11] two-way wireless communication,[12,13] and batteries with remote recharging capabilities.

Several studies have explored the use of microfabricated, etched, silicon columns for GC analysis of volatile organic compounds.[3,5,14−18] Columns prepared by deep reactive ion etching of silicon substrates and dynamically coated with nonpolar dimethyl polysiloxane and moderately polar trifluoropropylmethyl polysiloxane have been described.[19,20] These columns, when used

* Corresponding author. E-mail: rdsacks@umich.edu.
† University of Michigan.
‡ Sionex Corporation.

(1) Overton, E. B.; Carney, K. R.; Roques, N.; Dharmasena, H. P. *Field Anal. Chem. Technol.* **2001**, *5* (1−2), 97.
(2) Yu, C. M.; Lucas, M.; Koo, C.; Stratton, P.; DeLima, T.; Behymer, E. *Micro-Electro-Mechanical Systems (MEMS)* 1998; DSC Vol. 66, p 481.
(3) Noh, H.; Hesketh, P. J.; Frye-Mason, G. C. *J. Microelectromech. Syst.* **2002**, *11* (6), 718.
(4) Kolesar, E. D.; Reston, R. R. *IEEE Trans. Compon., Packag., Manuf. Technol.* **1998**, *21* (4), 324.
(5) Manginell, R. P.; Okandan, M.; Kottenstette, R. J.; Lewis, P. R.; Adkins, D. R.; Bauer, J. M.; Manley, R. G.; Sokolowski, S.; Shul, R. J. Monolithically Integrated μChemLab for Gas-Phase Chemical Analysis. In *Proc. Seventh Int. Conf. Miniaturized Chem. Biochem. Anal. Syst. − μTAS* '03; Squaw Valley, CA, October 5−9, 2003; p 1247.
(6) Santy, S.; Spilkin, A.; Strauss, J. *Am. Lab.* **1991**, *23*, 34.
(7) Smith, H.; Zellers, E. T.; Sacks, R. *Anal. Chem.* **1999**, *71*, 1610.
(8) Grall, A. J.; Zellers, E. T.; Sacks, R. D. *Environ. Sci. Technol.* **2001**, *35*, 163.
(9) Whiting, J. J.; Lu, C.-J.; Zellers, E. T.; Sacks, R. D. *Anal. Chem.* **2001**, *73*, 4668.
(10) Whiting, J.; Sacks, R. *Anal. Chem.* **2002**, *74*, 246.
(11) Lu, C.-J.; Whiting, J. J.; Sacks, R. D.; Zellers, E. T. *Anal. Chem.* **2003**, *75*, 1400.
(12) Kocer, F.; Walsh, P. M.; Flynn, M. P. Wireless, Remotely Powered Telemetry in 0.25 μm CMOS. *2004 VLSI Symposium*, Honolulu, HI, June 2004; p 24−27.
(13) Kocer, F.; Walsh, P. M.; Flynn, M. P. An Injection Locked, RF Powered, Telemetry IC in 0.25 μm CMOS. *IEEE Radio Freq. Integr. Circuits Conf. (RFIC 2004)*, Fort Worth, TX, June 2004; p 339−342.
(14) Matzke, C. M.; Kottenstette, S. A.; Casalnuovo, G. C.; Frye-Mason, G.; Hudson, M. L.; Sasaki, D. Y.; Manginell, R. P.; Wong, C. C. *Proc. 1998 SPIE Conf. Micromach. Microfabricat. Process Technol. IV*; p 262.
(15) Frye-Mason, G.; Kottenstette, R. J.; Lewis, P. R.; Heller, E. J.; Manginell, R. P.; Adkins, D. R.; Dullock, D.; Martinez, D.; Sasaki, D.; Mowry, C.; Matzke, C.; Anderson, L. *Proceedings of Micro Total Analysis Systems 2000*; Kluwer Academic Publishers: Dordrecht, The Netherlands, 2000; p 229.
(16) Potkay, J. A.; Driscoll, J. A.; Agah, M.; Sacks, R. D.; Wise, K. D. *Proc. 16th Ann. IEE Conf. Micro-Electro-Mech. Syst.* (MEMS), Kyoto, Japan, January 19−22, 2003; p 395.
(17) Agah, M.; Potkay, J.; Elstro, A.; Lambertus, G.; Sacks, R.; Wise, K. A high-performance temperature-programmed gas chromatography column. *North American Solid-State Sensors, Actuators, and Microsystems Workshop*, Hilton Head Island, SC, June 6−10, 2004; p 302−305.
(18) Zellers, E. T.; Steinecker, W. H.; Lambertus, G. R.; Agah, M.; Lu, C.-J.; Chan, H. K. L.; Potkay, J. A.; Oborny, M. C.; Nichols, J. M.; Astle, A.; Kim, H. S.; Rowe, M. P.; Kim, J.; Da Silva, L. W.; Zheng, J.; Whiting, J. J.; Sacks, R. D.; Pang, S. W.; Kaviany, M.; Bergstrom, P. L.; Matzger, A. J.; Kurdak, Ç.; Bernal, L. P.; Najafi, K.; Wise, K. D., A versatile MEMS gas chromatograph for environmental vapor mixture analysis. *Proceedings Solid-State Sensor, Actuator, and Microsystems Workshop*, Hilton Head Island, SC, June 6−10, 2004; p 61−66.

10.1021/ac051216s CCC: $30.25
Published on Web 00/00/0000

with air as carrier gas, typically generate 5000−8000 theoretical plates. A series-coupled ensemble of a nonpolar and polar microfabricated column recently has been used to achieve programmable selectivity.[20] Silicon etched GC columns generally have lower resolving power than conventional fused-silica wall-coated capillary columns, and thus, their use has been restricted to relatively simple mixtures.

Microfabricated GC columns operate efficiently under low volumetric flow rates and thus require detectors with very small residence times. Due to their simplicity and ease of fabrication, microfabricated thermal-conductivity detectors have been developed, but temperature constraints and poor minimum detectable limits can be problematic for some applications.[4,21,22] Selective detection to provide enhanced component identification and, in some cases, to provide for deconvolution of overlapping peaks in targeted analysis applications has received considerable attention to increase the utility of microfabricated columns. Notably, microfabricated arrays of polymer-coated surface acoustic-wave (SAW) devices[8,9,23] and chemiresistor devices[24,25] have been used as detectors for GC with microfabricated columns. Mixture characterization is based on pattern recognition.[24]

Conventional ion mobility spectrometers (IMS) have been used for the selective detection of volatile organic compounds.[26,27,28] Typically, these devices are operated in the time-of-flight (TOF) mode. Packets of ions, usually produced by atmospheric-pressure chemical ionization (APCI),[26,29] are electronically gated into a region containing a linear electric field, and their TOF to an ion collector is measured. A relatively large gas flow opposite in direction to the ion flight is used. Low duty cycle, ion cluster formation, and restriction to only positive or negative ion collection in a single experiment are significant limitations. In addition, IMS does not scale well, and microfabricated devices have shown relatively poor performance.[30,31]

Recently, a novel microfabricated mobility-based detector (differential mobility spectrometer, DMS) with high selectivity and excellent detection limits for many volatile organic compounds has been described.[32−36] With DMS, an asymmetric radio frequency (RF) electric field is applied between a pair of metallic electrodes. At low electric field strength, ion mobility is relatively field-independent. For high field strength, (greater than ~10 kV/cm), ion mobility may show strong field dependence. For DMS, the field oscillates between a high field and a low field value, and the difference in mobility determines the ion trajectory through the detector cell. Ions with an appropriate differential mobility pass through the cell, and a pair of biased collector electrodes collect both positive and negative ions from the same experiment. A DC compensation voltage applied to one of the RF plates is scanned to allow ions with different differential mobility to pass through the cell without being annihilated at the plates. Data are displayed as ion current versus compensation voltage and analysis time. Separate readout channels are provided for positive and negative ions. In addition to collecting positive and negative ions in the same experiment, advantages of DMS include greater resolving power, higher duty cycle, reduced ion cluster formation, and excellent scaling for microfabricated devices relative to conventional IMS.

For the studies described here, a 3.0-m-long etched, silicon, microfabricated column which generates about 5500 theoretical plates is combined with a commercial DMS detector (model SVAC-V, Sionex Corp., Bedford, MA) and evaluated for the analysis of volatile organic compounds. The DMS uses a ^{63}Ni ionization source with nitrogen as the transport gas and air as the column carrier gas. Data are presented for compounds containing a variety of functional groups which illustrate the formation and detection of both positive and negative ions. The effects of RF voltage and detector temperature on detector selectivity and ion-cluster formation are evaluated.

EXPERIMENTAL SECTION

Apparatus. Figure 1 shows the experimental system used for this study. A Varian 3400 capillary GC with a split inlet I and flame ionization detector, FID, was used as a platform for column temperature programming and sample injection. The FID was used for comparison with the DMS detector. For DMS detection, a 30-cm-long, 0.1-mm-i.d. segment of deactivated fused-silica tubing passed from the downstream end of the column through the GC wall and was plumbed into the high-velocity flow of dry nitrogen entering the ionization region of the DMS. The connection line was wrapped with heating wire and heated to 120 °C to reduce band broadening contributions. The sample residence time in the microfabricated detector cell is about 1 ms, and the device appears to contribute no significant instrumental dead time to the system.

For DMS transport gas, house nitrogen was purified using hydrocarbon and moisture traps and passed through a coil of copper tubing immersed in a Dewar of liquid nitrogen. The nitrogen flow rate was set at 300 cm^3/min by means of a flow controller in the DMS unit. House air was used for column carrier gas after purification with filters for water vapor and hydrocarbons. Carrier gas flow rate was 0.25 cm^3/min as calculated at the column outlet.

Column Design. Columns were etched as 150-μm-wide by 240-μm-deep rectangular channels in silicon substrates. The

(19) Lambertus, G.; Elstro, A.; Sensenig, K.; Potkay, J.; Agah, M.; Scheuering, S.; Wise, K. D.; Dorman, F.; Sacks, R. *Anal. Chem.* **2004**, *76*, 2629.
(20) Lambertus, G.; Sacks, R. *Anal. Chem.* **2005**, *77*, 2078.
(21) Wu, Y. E.; Chen, K.; Chen, C. W.; Hsu, K. H. *Sens. Actuators. A* **2002**, *100*, 37.
(22) Chen, K.; Wu, Y. E. *Sens. Actuators. A* **2000**, *79*, 211.
(23) Bender, F.; Barie, N.; Romoudis, G.; Voigt, A.; Rapp, M. *Sens. Actuators, B* **2003**, *93*, 135.
(24) Steinecker, W. H.; Rowe, M. P.; Matzger, A. J.; Zellers, E. T. Chemiresistor array with nanocluster interfaces as a micro-GC detector. In *Proceedings of the 12th International Conference on Solid-State Sensors, Actuators and Microsystems, Transducers '03*, Boston, MA, June 8−12, 2003; p 1343.
(25) Cai, Q.-Y.; Zeller, E. T. *Anal. Chem.* **2002**, *74*, 3533.
(26) Eiceman, G. A.; Karpas, Z. *Ion Mobility Spectrometry*; CRC Press: Boca Raton, FL 1994.
(27) Ewing, R. G.; Atkinson, D. A.; Eiceman, G. A.; Ewing, G. J. *Talanta* **2001**, *54*, 515.
(28) Collins, D. C.; Lee, M. L. *Anal. Bioanal. Chem.* **2002**, *372*, 66.
(29) Borsdorf, H.; Nazarov, E. G.; Eiceman, G. A. *Mass Spectrom.* **2004**, *232*, 117.
(30) Xu, J.; Whitten, W. B.; Ramsey, J. M. *Anal. Chem.* **2000**, *72*, 5787.
(31) Longwitz, R. G.; Lintel, H. V.; Renaud, P. *J. Vac. Sci. Technol., B* **2003**, *21*, 1570.
(32) Miller, R. A.; Eiceman, G. A.; Nazarov, E. G.; King, T. A. A MEMS Radio Frequency Ion Mobility Spectrometer for Chemical Agent Detection. *Solid-State Sensor and Actuator Workshop*, Hilton Head Island, SC, June 4−8, 2000.
(33) Eiceman, G. A.; Tadjikov, B.; Krylov, E.; Nazarov, E. G.; Miller, R. A.; Westbrook, J.; Funk, P. *J. Chromatogr., A.* **2001**, *917*, 205.
(34) Eiceman, G. A.; Krylov, E. V.; Tadjikov, B.; Ewing, R. G.; Nazarov, E. G.; Miller, R. A. *Analyst* **2004**, *129*, 297.
(35) Eiceman, G. A.; Krylov, E. V.; Krylova, N. S. *Anal. Chem.* **2004**, *76*, 4937.
(36) Miller, R. A.; Nazarov, E. G.; Krylova, N. S.; King, A. T. *Anal. Chem.* **2001**, *91*, 301.

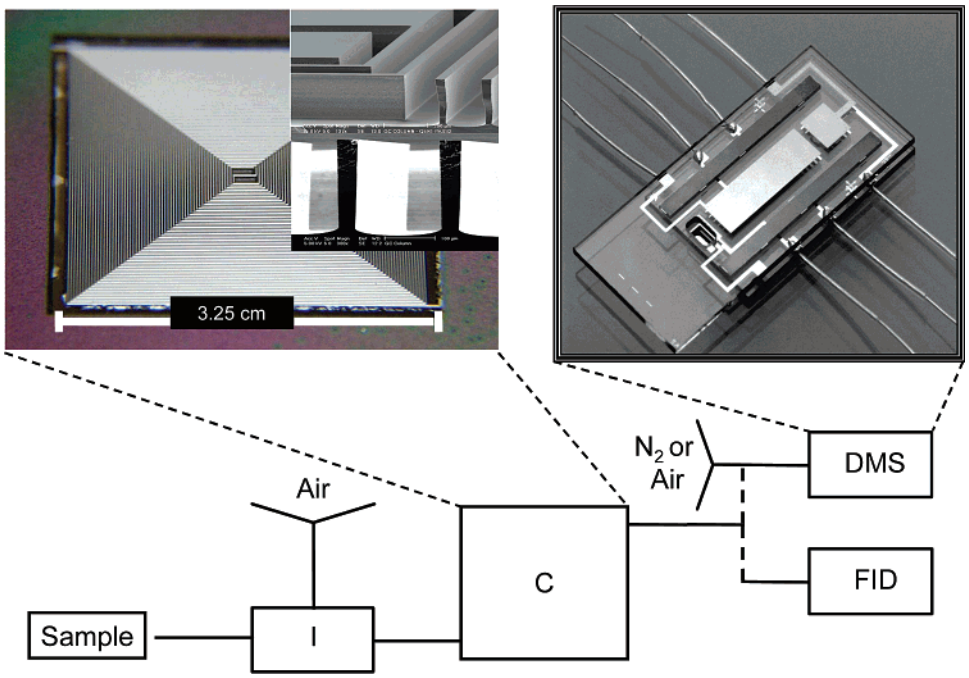

Figure 1. Apparatus showing details of the microfabricated column (upper left inset) and the microfabricated DMS cell (upper right inset). A Varian 3400 GC is used as a platform. I, split inlet; FID, flame ionization detector; C, microfabricated column. The two detectors can be used alternately.

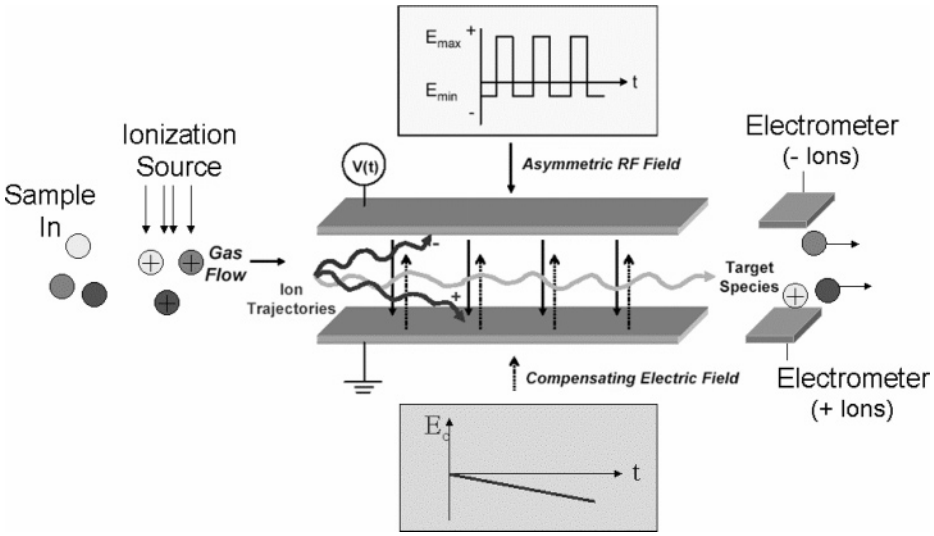

Figure 2. Operation of a radio frequency differential mobility spectrometer.

rectangular cross section of the channel was created by deep reactive ion etching. The column used was a 3-m-long channel etched as a double square spiral in a 3.2 cm × 3.2 cm chip. Four columns were simultaneously etched in a 4-in. silicon wafer. A Pyrex wafer was anodically bonded to the top of the silicon wafer, forming the fourth wall of the closed channel. The column is shown as an inset in the upper left corner of Figure 1. Structure of the etched channel is illustrated in the upper right corner of the inset. Etched ports in the upper left and lower right corners of the chip were used to connect 0.1-mm-i.d. fused-silica tubing to the chip by means of an epoxy seal.

The channel walls were coated with nonpolar dimethyl polysiloxane by means of a dynamic coating process in which a plug of the coating solution is pushed through the channel at a controlled velocity with pressurized nitrogen. Gas flow continues as the solvent gradually evaporates from the thin film on the inner wall of the channel. The stationary phase is cross-linked in an oven by a thermally activated catalyst. The column is tested with a standard mixture before and after cross linking.[19] Stationary phase film thickness was not measured and is predicted to be >1 μm, since a relatively high-viscosity coating solution was used to minimize possible sagging of the film on the vertical channel walls before solvent evaporation is complete.[37]

DMS Design. The differential mobility spectrometer is composed of an ionization region, which houses a 5-mCi ^{63}Ni ionization source, a tunable ion filter, and collector electrodes, as seen in Figure 2. Ions formed in the ionization region due to APCI are passed by a transport gas through the ion filter region composed

(37) Grob, K. *Making and Manipulating Capillary Columns for Gas Chromatography*; Dr. Alfred Huthig Verlag: Heidelberg, 1986.

Table 1. Compounds Used in the Test Mixture

no.	component	no.	component
1	pentane	24	propyl benzene
2	methyl sulfide	25	iodomethane
3	isopropyl alcohol	26	ethyl bromide
4	acetonitrile	27	dichloromethane
5	propionitrile	28	carbon disulfide
6	ethyl acetate	29	iodoethane
7	*tert*-butyl ethyl ether	30	chloroform
8	tetrahydrofuran	31	bromopropane
9	benzene	32	1,1,1-trichloroethane
10	3-methyl-2-butanone	33	1,2-dichloropropane
11	thiophene	34	iodopropane
12	ethylene glycol dimethyl ether	35	bromobutane
13	2-pentanone	36	1,3-dichloropropene
14	2-ethylfuran	37	1-chloropentane
15	4-methyl-2-pentanone	38	1-iodo-2-methyl propane
16	toluene	39	chlorodibromomethane
17	2-hexanone	40	tetrachloroethylene
18	butyl acetate	41	iodobutane
19	ethyl benzene	42	1-chlorohexane
20	*m*-xylene	43	bromoform
21	cyclohexanone	44	1,1,2,2-tetrachloroethane
22	*o*-xylene	45	iodopentane
23	bromobenzene		

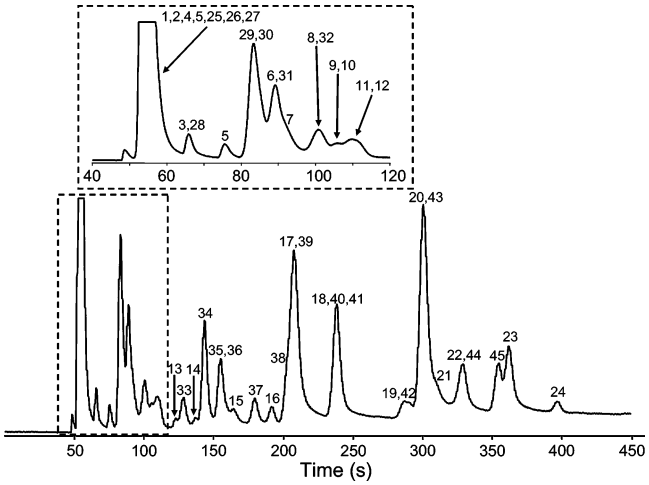

Figure 3. Chromatogram of the 45-component test mixture described in Table 1 using the 3.0-m-long microfabricated silicon column with FID detection. Peak numbers correspond to the compound numbers in Table 1.

of two planar electrodes separated by an analytical gap. The electrode dimensions are 15 mm × 1.5 mm, and the gap is 0.5 mm. Filtered ions are detected downstream from the filter by two electrodes connected to detection circuits that measure the induced ion current. As ions move with the transport gas flow, both positive and negative ions can be filtered simultaneously and detected by corresponding detector electrodes. Ion filtering is produced by the superposition of two electric fields, a high frequency ~1.2-MHz RF field with an associated voltage variable from −500 to 1500 V and a compensation voltage. The compensation voltage can be ramped from approximately −40 to +15 V and is synchronized with the data collection system to generate a plot of ion current intensity versus compensation voltage.[36] Depending on the analytes of interest, the scan range and the voltage step size can be tailored to allow for faster scan rates or to provide longer collection times during each step of a scan.

Materials and Procedures. The test mixture used to compare FID detection with DMS detection for the microfabricated column is described in Table 1. The 45-component mixture contains volatile organic compounds with a variety of functional groups, including aromatics, organic chlorides, bromides, and iodides, as well as oxygen-, nitrogen-, and sulfur-containing compounds. Retention times for the conditions used here were measured using injections of the individual components or simple, completely resolved mixtures. Mixtures in pentane at various concentrations were made by dilutions of stock solution. For most DMS studies, concentrations were calculated to be in the 1−100 ppb range (vol/vol) in the detector cell. Injection volumes were typically 1.0 μL with a split ratio of 600:1. For most studies, the column temperature was programmed from 30 to 120 °C at 10 °C/min.

The DMS has an on-board heater, and the detector temperature was varied as needed. For this study, temperatures in the range 30 to 120 °C were evaluated. The RF voltage is user-adjustable and -programmable. Values in the range from 800 to 1500 V were used in this study. The scanning range of the compensation voltage is programmable, and scanning parameters were adjusted as needed. Data from the DMS as ion current versus compensation voltage and analysis time are logged directly into Excel spreadsheets with independent data sets logged simultaneously from the positive and negative ion channels.

RESULTS AND DISCUSSION

System Operation. Figure 3 shows a chromatogram obtained from the 45-component test mixture described in Table 1 using a 3.0-m-long microfabricated column with FID detection. Peak numbers correspond to component numbers in Table 1. The portion of the chromatogram in the dotted-line box is shown on an expanded time scale above the main chromatogram. The test mixture elutes over the volatility range from *n*-C_5 to *n*-C_{10} with the nonpolar stationary phase. The chromatogram is complete in about 400 s, but only a few components are adequately resolved for quantitative measurements. The column generates ~5500 theoretical plates using air carrier gas at an average linear velocity of 10.8 cm/s. The pentane solvent peak is very intense and masks peaks from several target compounds.

Figure 4 shows the two-dimensional contour plot of electrometer output for the positive ion channel (left panel) and the negative ion channel (right panel) from the DMS using the same column and separation conditions as for Figure 3. The vertical axis is the time after sample injection, and the horizontal axis is the DMS compensation voltage. The display color indicates peak amplitude. The RF voltage for the DMS was 1300 V, and the detector temperature was 100 °C. The compensation voltage was scanned from +10 to −35 V at 1 Hz. Note that there is a substantial portion of the compensation voltage scan for which both positive and negative ions are collected.

The enhancement in information content in the two-dimensional data in Figure 4 relative to the one-dimensional chromatogram in Figure 3 is remarkable. The peak capacity of the microfabricated column combined with DMS detection is dramatically increased, and a distinct if not completely separated peak is observed for each of the 45 components in the test mixture. Peak widths along the compensation voltage axis are typically 2.5 V (base width). For this mixture, peaks are observed on the positive

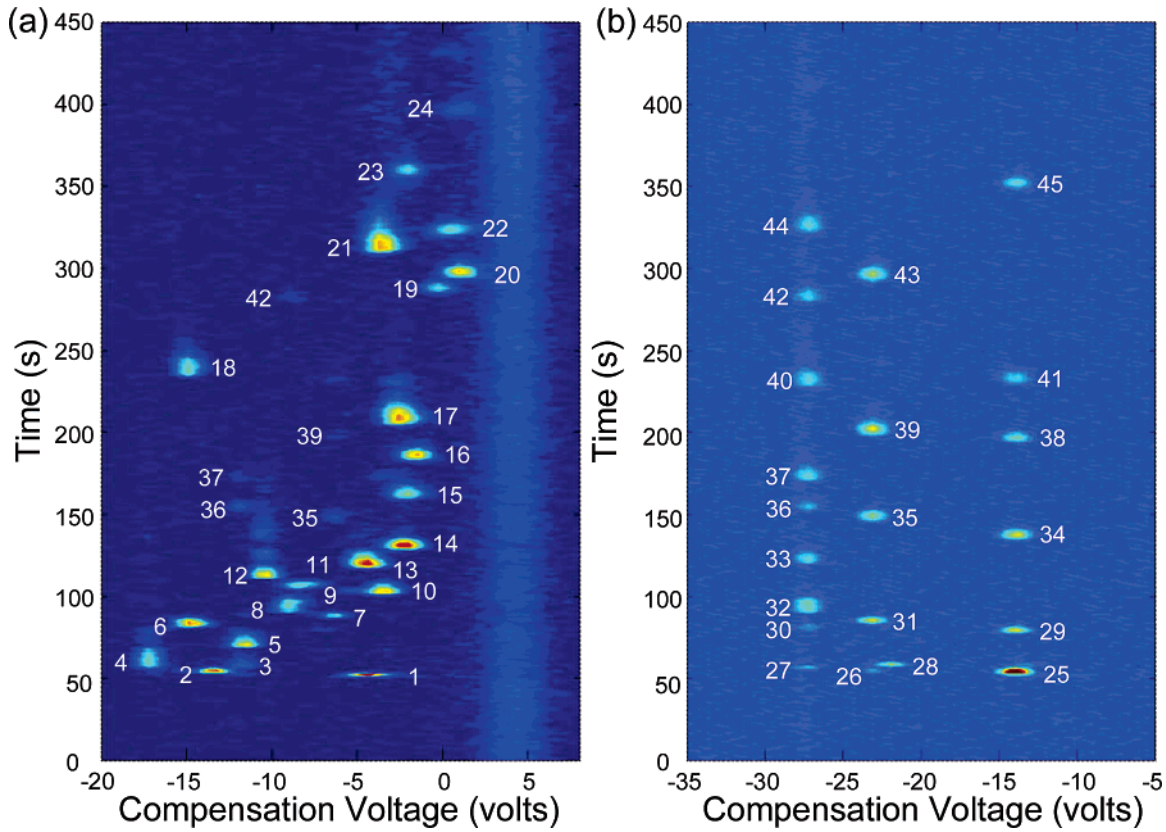

Figure 4. Contour plots for the 45-component test mixture from the microfabricated column-DMS system. The contours show ion current (contour color) as a function of retention time (vertical axis) and compensation voltage (horizontal axis) for the positive ion channel (a) and the negative ion channel (b).

ion channel for compensation voltages in the range 0 to −20 V and on the negative ion channel for compensation voltages in the range −10 to −30 V. This gives a peak capacity of ~8 peaks for each channel or a total of ~16 peaks. The holdup time of the column is ~32 s, and the last peak of interest (peak 24) elutes in 400 s. From this, the column peak capacity for a resolution of 1.5 is ~29 peaks. This gives a total peak capacity of ~464 peaks for the two-dimensional display. However, a component can produce multiple ion peaks either from fragmentation of the parent molecule or clustering of ionized species.

The positive ion channel shows peaks for 28 of the target compounds and the pentane solvent (peak 1). Note that *n*-pentane and other low-molecular-weight saturated hydrocarbon compounds are not detected at low concentrations with APCI. Thus, the solvent does not produce a large and very wide peak as it did in the FID chromatogram shown in Figure 3. Positive ion peaks are randomly distributed over a wide range of compensation voltages. In general, higher-molecular-weight compounds show a smaller range of compensation voltages than the lower-molecular-weight compounds. This is useful for GC detection, since volatile compounds often are more difficult to separate due to inadequate interaction with the stationary phase in the column. A high-molecular-weight compound that exhibits an unusually negative compensation voltage is butyl acetate (peak 18). Note that both butyl acetate and ethyl acetate (peak 6) are observed with a compensation voltage of −15 V. This is likely due to the formation of acetate ions produced from fragmentation of the parent molecules during the ionization process.

The appearance of the negative ion channel plot contrasts with the positive channel plot in that peaks tend to form vertical patterns. That is, there are three groups of peaks with different retention times but similar compensation voltages. Peaks 27, 30, 32, 33, 36, 37, 40, 42, and 44 are all chloride compounds with a chlorine attached to an aliphatic carbon. These compounds produce peaks with compensation voltage centered near −27.5 V. Peaks 26, 31, 35, 39, and 43 are all from aliphatic brominated compounds, and all have peaks with the central compensation voltage of about −23 V. Note that compound 39 is from chlorodibromomethane, but no peak is produced at 27.5 V, despite the fact that the compound contains aliphatic chlorine. Peaks 25, 29, 34, 38, 41, and 45 are all aliphatic iodides, and all produce peaks with compensation voltage centered near −14 V. The only other major peak observed in the negative ion channel is peak 28 from carbon disulfide, which is a frequently used extraction solvent. Eliminating this as a possible interference in the analysis of volatile compounds will be useful.

For a few of these halogenated aliphatic compounds (peaks 35, 36, 37, 39, and 42), low amplitude peaks are observed on the positive ion channel as well as the large peaks on the negative ion channel. Bromobenzene, the only aromatic halogen compound in the test mixture, only produces a peak on the positive ion channel. Other data have shown that aromatic compounds with a single halogen atom appear only in the positive ion channel. Aromatic compounds with multiple halogen atoms do produce strong peaks on the negative ion channel. This suggests that there is a stronger bond between the aromatic ring structure and the

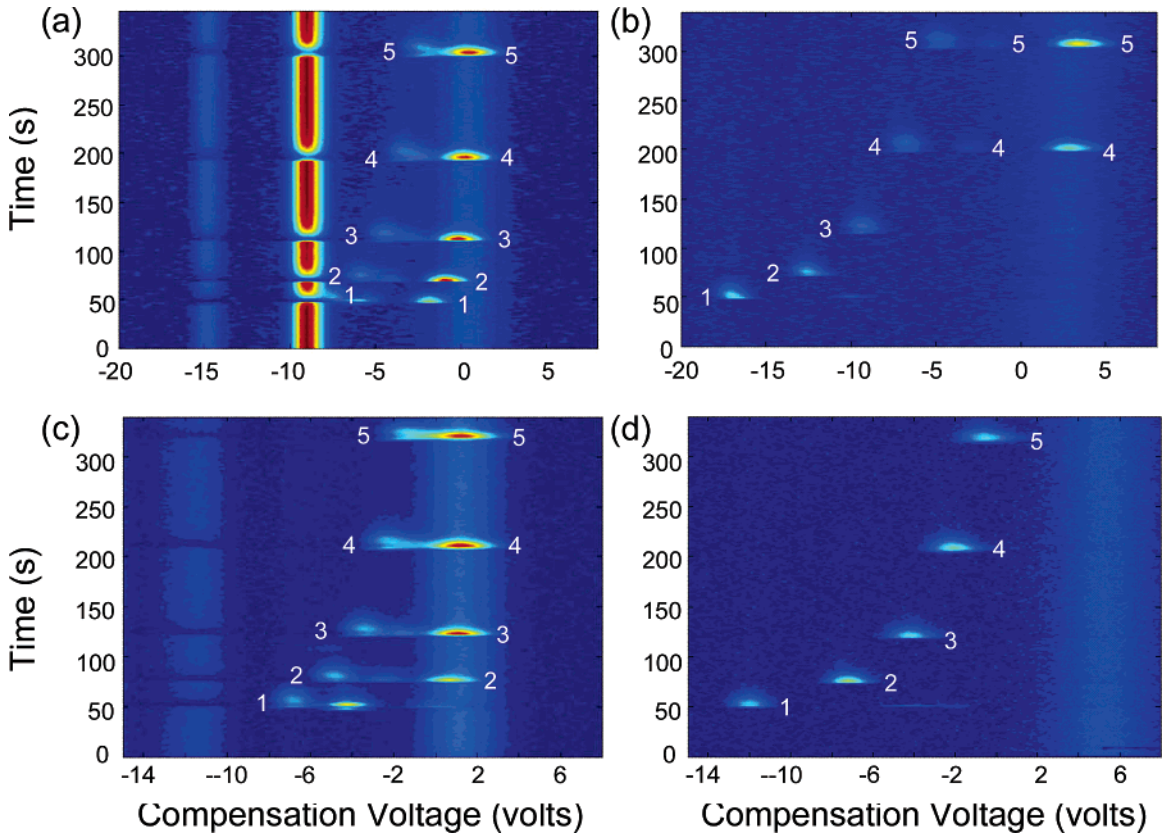

Figure 5. Contour plots for a homologous series of ketones from the microfabricated column-DMS system. The contours show ion current (contour color) as a function of retention time (vertical axis) and compensation voltage (horizontal axis) for the positive ion channel. (a) Detector temperature 50 °C and RF voltage 900 V; (b) 100 °C and 900 V; (c) 50 °C and 1400 V; (d) 100 °C and 1400 V. Peaks labeled 1−5 are for acetone, 2-butanone, 2-pentanone, 2-hexanone, and 2-heptanone, respectively.

first halogen atom than with any additional halogen atoms or between halogen atoms and an aliphatic hydrocarbon structure. The result is that single halogens on an aromatic ring are not as easily cleaved as other halogens.

Note that peaks 25, 26, and 27 from iodomethane, ethyl bromide, and dichloromethane, respectively, show very little retention despite the relatively thick stationary phase used in the microfabricated column to increase retention. These highly volatile compounds could not be separated by the column, even without the presence of the high concentration of the pentane solvent, but are easily separated with the DMS.

Since the same compensation voltage is observed for most aliphatic chlorides, it is likely that the same chemical species is detected for all of these compounds. The same is true for the aliphatic bromides and iodides. The most likely species are the halogen ions Cl^-, Br^- and I^-, respectively or adduct species of these ions with the transport gas. This feature of the DMS is unique and very useful for the identification of these compounds.

Temperature and RF Voltage. An important advantage of differential mobility devices is that they operate at higher field strengths, as compared with conventional time-of-flight ion mobility spectrometers. The higher field strengths (or RF voltages) used in the DMS can significantly reduce the amount of ion cluster formation, which can be a major problem with conventional time-of-flight ion mobility as it degrades analyte resolution. Figure 5 shows the positive ion channel for a homologous series of ketones separated with the microfabricated column. The panel in the upper left was obtained with a detector temperature of 50 °C and an RF voltage of 900 V. The panel in the lower left was obtained with the same RF voltage and a temperature of 100 °C. The two right-hand panels were obtained at the same two temperatures but with an RF voltage of 1400 V. Peaks labeled 1−5 correspond to the homologous series of ketones. In some cases, multiple peaks are observed.

In the upper left panel, the two vertical ridges, one showing high intensity at a compensation voltage of about −9 V, and the other at −15 V with much lower amplitude are believed to be reactant ions of nitrogen and trace levels of water in the transport gas. Note that these ridges have voids in them corresponding to the retention times of the ketones. This is the result of charge transfer from the reactant ions to sample molecules as they pass through the ionization region of the device and pick up the charge from the reactant ions. If the detector temperature is increased from 50 to 100 °C (lower left panel), the high-intensity vertical ridges completely disappear. Ion mobility increases with temperature, and the amplitude of ion oscillation induced by the RF field will therefore increase. This results in ions hitting the filter electrodes and being neutralized within a few RF cycles. The reactant ions typically have significantly higher mobility than ionized sample species, and as a result, the reactant ion peak may disappear but analyte peaks still remain at elevated temperatures.

When the RF voltage is increased to 1400 V, there is no detected reactant ion for either detector temperature. Either the higher voltage increases the amplitude of ion oscillation sufficiently so that the reactant ions are annihilated at the electrodes or their compensation voltage is shifted to a value beyond the range used

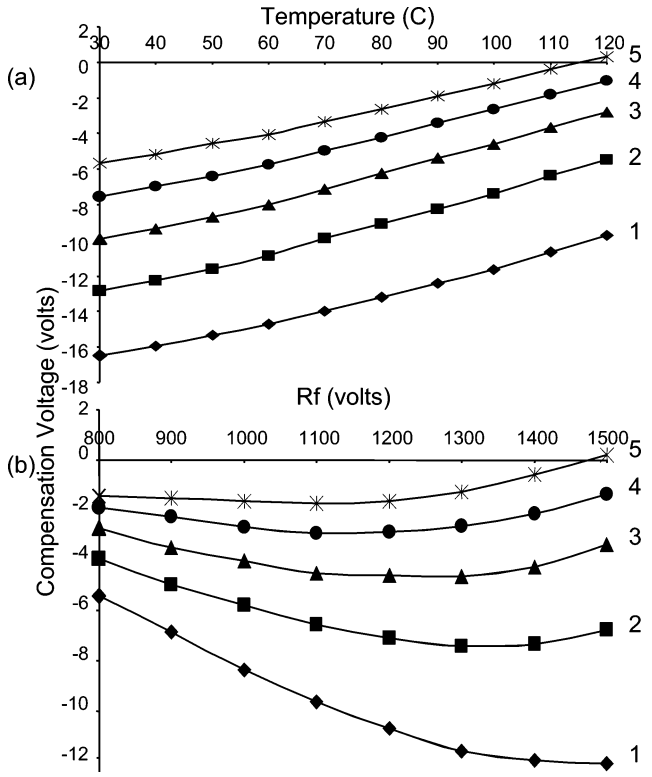

Figure 6. Plots of compensation voltage as a function of detector temperature for an RF voltage of 1300 (a) and as a function of RF voltage for a detector temperature of 100 °C (b) for the ketone homologous series from Figure 5. Plots labeled 1−5 are for acetone, 2-butanone, 2-pentanone, 2-hexanone, and 2-heptanone, respectively.

in this study. With the 1400-V RF and a detector temperature of 50 °C (upper right panel), significant cluster ion signal is observed, particularly for the higher-molecular-weight homologues . From previous experimentation, the peak to the left is believed to be primarily associated with the monomer, whereas the peak closer to zero compensation voltage is believed to be a dimer peak. For a RF voltage of 1400 V and a detector temperature of 100 °C (lower right panel), there are no detectable cluster peaks, and one well-defined peak per compound is observed. Note that the compensation voltage for these ketones is dispersed from 0 to −12 V, with the lowest-molecular-weight species having the most negative voltage. Other homologous series of positive ion-producing compounds often show similar qualitative results with the higher-molecular-weight homologues having smaller negative compensation voltages and reduced molecular-weight dispersion along the compensation-voltage axis.

Figure 6 shows plots of compensation voltage as a function of detector temperature at a fixed RF voltage of 1300 V (a) and as a function of RF voltage at a detector temperature of 100 °C (b) for the same homologous series of ketones. In all cases, acetone (plots labeled 1) has the largest negative compensation voltage. The higher-molecular-weight homologues have progressively smaller negative compensation voltages, and for 2-heptanone, at the highest temperature and the highest RF voltage values, the compensation voltage becomes positive.

The data of compensation voltage versus detector temperature gives relatively linear, parallel plots for the homologous series. Note that the shift in compensation voltage over the 90 °C

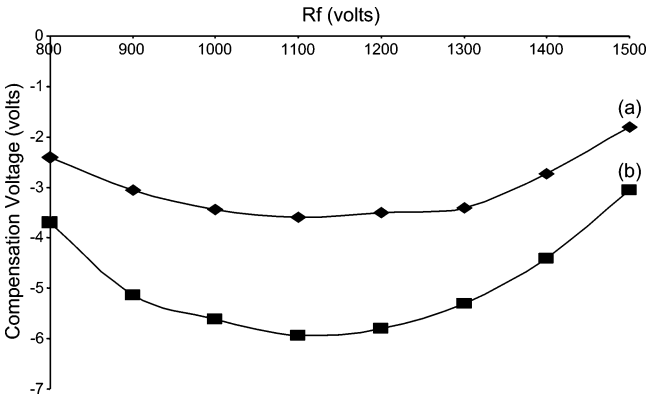

Figure 7. Plots of compensation voltage versus RF voltage for 3-methyl-2-butanone (a) and benzene (b).

temperature range shown in the plots is ∼6 V. The slopes of these plots show a temperature sensitivity of the compensation voltage to temperature of ∼0.07 V/°C. This should be compared with the peak widths of ∼1 V full width at half-maximum amplitude to ascertain the detector temperature control needed for a given application.

The plots in Figure 6b show the effects of RF voltage on compensation voltage for the homologous series of ketones. Plots of this type directly show the effects of RF voltage on differential ion mobility and are unique for every chemically unique species. For the ketones, the compensation voltage becomes more negative as the RF voltage increases, and the largest change occurs for the lowest-molecular-weight homologues.

Each plot goes through a minimum, and at sufficiently high RF voltages, the compensation voltage becomes less negative with increasing RF voltage. These minimums in the plots are shifted to lower RF values as the molecular weights of the homologues increase. Note that the dispersion of peaks along the compensation voltage axis increases with increasing RF voltage. Since peak widths appear to show only a weak dependence on RF voltage, higher RF voltages may be preferred to increase peak capacity along the compensation voltage axis and to substantially reduce ion cluster formation.

Tunable Selectivity. Since the effects of RF voltage on compensation voltage are unique for every ionic species, in some cases, it is possible to tune the compensation voltage to enhance the separation of components that coelute from the separation column. A good example is found for components 9 (benzene) and 10 3-methyl-2-butanone from Table 1. The column retention times for these components are 120.6 and 124.3 s, and the average baseline peak width is 10.0 s. This gives a chromatographic resolution of 0.37.

Figure 7 shows plots of compensation voltage versus RF voltage for these two compounds. At the lowest RF value of 800 V, the peak separation on the compensation voltage scale is ∼1.30 V. Assuming an average peak width (4σ) of ∼2.5 V and near Gaussian peak shape, the corresponding resolution is ∼0.50. Similar resolution is obtained at the highest RF voltage used in this study (1500 V). For an RF voltage of 1100 V (value of greatest separation in Figure 7), the separation is 2.34 V, and the corresponding resolution is increased to 0.94.

Figure 8 shows contour plots for components 9 and 10 on expanded retention time and compensation voltage axes. Plots

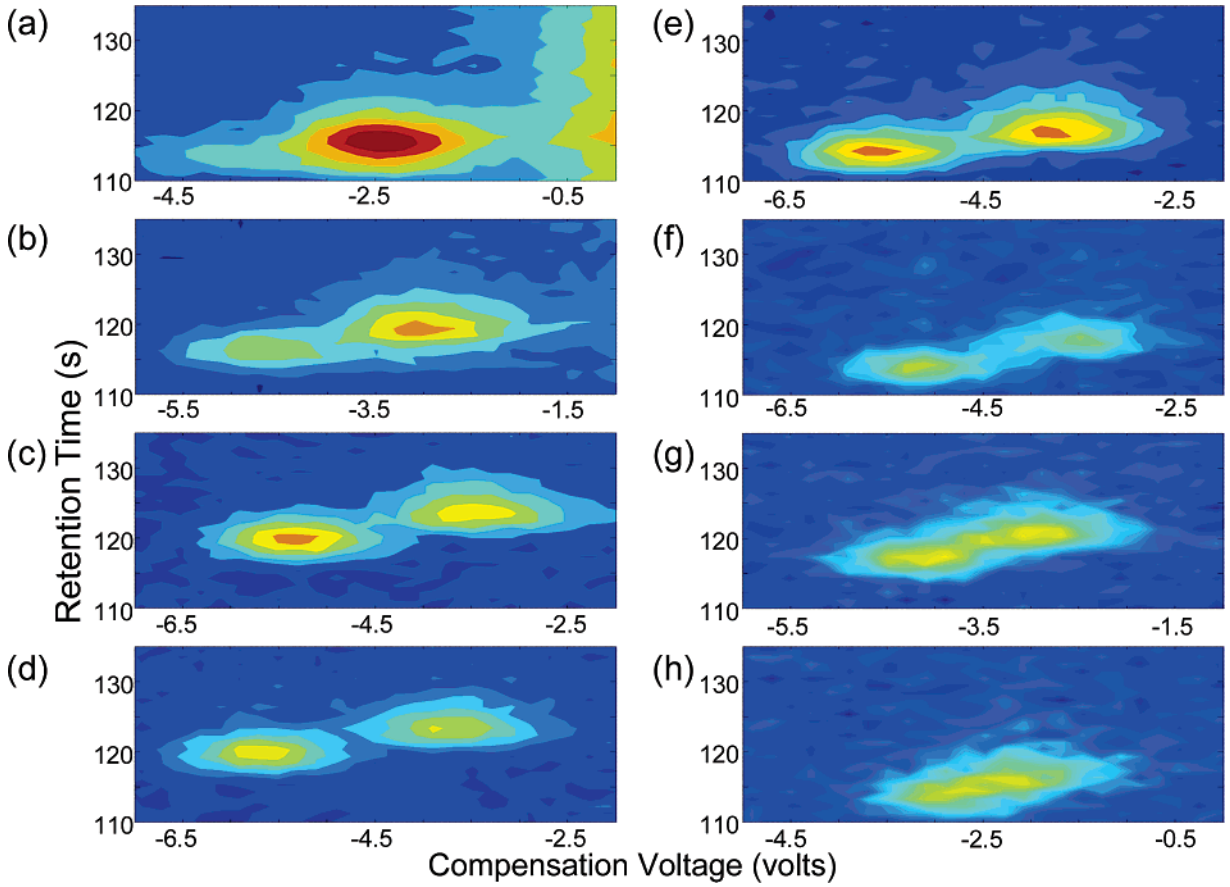

Figure 8. Contour plots for 3-methyl-2-butanone and benzene for RF voltages of 800 (a), 900 (b), 1000 (c), 1100 (d), 1200 (e), 1300 (f), 1400 (g), and 1500 V (h). The left peak is benzene and the right peak is 3-methyl-2-butanone. The detector temperature was 100 °C.

are shown for RF voltages in 100-V increments from 800 (a) to 1500 V (h), respectively. Note that the compensation voltages change with changing RF voltages (Figure 7), so different ranges are shown for different plots, but the scale is the same for all plots.

For the lowest RF voltage (a), only a single, broadened and distorted peak is observed. When the RF voltage is increased to 900 V (b), a substantial shift in compensation voltage is observed, and the shoulder appears to the left of the principal peak. For RF voltages in the range 1000−1200 V (c−e), two peaks are clearly seen. For an RF voltage of 1100 V, the resolution along the compensation voltage axis is 0.94, and the overall resolution is slightly greater due to the chromatographic resolution of 0.37. For an RF voltage of 1300 V, the peaks for the two components begin to coalesce. This trend continues at 1400 V, and at 1500 V, only a single, broad and distorted peak is observed. Optimizing the RF voltage for resolution alone will not be ideal for all situations, because the RF voltage affects both resolution (Figure 8) and cluster peak formation (Figure 5); sacrificing resolution of a specific component pair to reduce ion cluster formation can allow for more effective utilization of the available peak capacity throughout the analysis.

CONCLUSIONS

The combination of a silicon microfabricated column and a silicon microfabricated differential mobility spectrometer has led to a very powerful analysis tool for volatile organic compounds. The burden of selectivity is shared between the column and the detector. A very large peak capacity has been achieved in a relatively short analysis time using two microfabricated devices. Because of the relatively high gas flow through the detector cell and the ionization region, the detector results in no significant extra-column band broadening, despite the relatively low volumetric flow through the column. The possibility of integrating the column and the detector on a single silicon substrate is under investigation and will eliminate extra-column band broadening from connection lines.

The DMS is a very useful GC detector due to high selectivity for many organic compounds. The ability of the device to simultaneously collect data on positive and negative ions is noteworthy. The properties of the detector and of APCI result in very telltale patterns of peaks for many halogenated compounds, and the group separation of these compounds from most other compounds, which are detected on the positive ion channel, and the further speciation of these ubiquitous compounds along the compensation-voltage axis are very useful qualitative features of the device.

The RF voltage is probably the most useful parameter for the control of the detector selectivity and of the resulting pattern of peaks observed in the two-dimensional data sets obtained from the DMS-microfabricated column combination. Higher RF voltages may be preferred due to reduced ion cluster formation as well as greater dispersion of component peaks along the compensation voltage axis. Since the RF voltage is programmable, it can be adjusted on the fly during a separation to enhance the DMS peak

resolution for targeted components that coelute from the microfabricated column. The quantitative analysis features of the microfabricated column-DMS detector instrument will be discussed in future reports.

ACKNOWLEDGMENT

The authors express their appreciation to Dr. Ken Wise, Mr. Masoud Agah, and Mr. Joseph Potkay at the University of Michigan Electrical Engineering and Computer Science Department for fabrication of the columns. Funding for this work was provided by the University of Michigan Center for Wireless Integrated Microsystems (WIMS) through the Engineering Research Centers Program of the National Science Foundation under Award no. ERC-9986866. Additional support was provided by Grant R01-OH03692 from the National Institute for Occupational Safety and Health of Centers for Disease Control and Prevention (NIOSH-CDCP).

Received for review July 8, 2005. Accepted September 20, 2005.

AC051216S